

Monte Carlo and mean-field study of antiferromagnetic ordering in cupric oxides

Weige Xue, Gary S. Grest, Morrel H. Cohen, and Sunil K. Sinha

Corporate Research Science Laboratory, Exxon Research and Engineering Company, Annandale, New Jersey 08801

Costas Soukoulis

Ames Laboratory and Department of Physics, Iowa State University, Ames, Iowa 50011

(Received 11 April 1988)

We have carried out simulations of the magnetic properties of undoped La_2CuO_4 , using a classical Heisenberg model for the Cu spin with a strong antiferromagnetic coupling J_0 in the a - c plane and weak interplane couplings. In the orthorhombic state, the coupling between nearest-neighbor spins in the b - c and a - b planes are not equal. We found that the antiferromagnetic-to-paramagnetic transition temperature (Néel temperature) depends only on the difference of these two interactions, ΔJ . For $\Delta J > 0.1 |J_0|$, T_N depends nearly linearly on ΔJ . When compared with the results of ordinary mean-field as well as a renormalized mean-field theory, our Monte Carlo simulation gives a substantially lower T_N for $\Delta J \gtrsim 0.025 |J_0|$. The relation between T_N and ΔJ of a three-dimensional simple cubic lattice with in-plane antiferromagnetic interaction J_0 and interplane coupling ΔJ is also calculated using low-temperature spin-wave theory. The spin-wave calculation gives a better estimate of T_N compared with our simulation results than the two mean-field-theory results.

I. INTRODUCTION

The magnetic ordering of the Cu spins into an antiferromagnetic, long-range ordered state in La_2CuO_4 has recently been confirmed by a number of neutron scattering studies.¹⁻⁴ While it has been proposed that magnetism may play an important role in high-temperature superconductivity in the $\text{La}_{2-x}\text{Sr}_x\text{CuO}_4$ and $\text{YBa}_2\text{Cu}_3\text{O}_{6+x}$ families of materials, the study of magnetic ordering in La_2CuO_4 is interesting in its own right. This system is highly anisotropic with a very strong coupling between Cu spins in the plane and very weak coupling between planes. The system undergoes a tetragonal to orthorhombic transition at a temperature greater than the Néel temperature T_N . In the antiferromagnetic (AF) state, the structure shown in Fig. 1 consists of Cu moments pointing "up" and "down" in succession in planes normal to the orthorhombic [100] axis, with the moment directions freezing along the orthorhombic [100] axis. Thus this system has interesting magnetic properties which may be representative of a wider class of quasi-two-dimensional antiferromagnetics. For this reason, we decided to carry out a detailed study of the magnetism of a classical Heisenberg model with interactions in the range appropriate to the cupric oxides.

Since the Néel temperature can be quite high [~ 200 – 250 K (Refs. 1–5)] depending on oxygen deficiency, we decided to model the system with a classical Heisenberg spin at each Cu spin. The interaction in the CuO plane is quite large (~ 1300 K).⁵ In the high-temperature tetragonal state, the interaction between nearest-neighbor spins in the b - c and a - b planes are equal and there can be no long-range magnetic ordering, even though the spin-correlation length in the a - c plane can become quite large. As the temperature is reduced, a transition occurs and the system transforms to an ortho-

rhombic structure in which the lattice constant c becomes greater than a . In this state, the magnetic interaction J_1 is larger than J_2 , and the system has long-range magnetic ordering below T_N in the state shown in Fig. 1. Since the in-plane interaction is large, a weak net coupling $\Delta J = |J_1| - |J_2|$ can produce a large change in T_N .

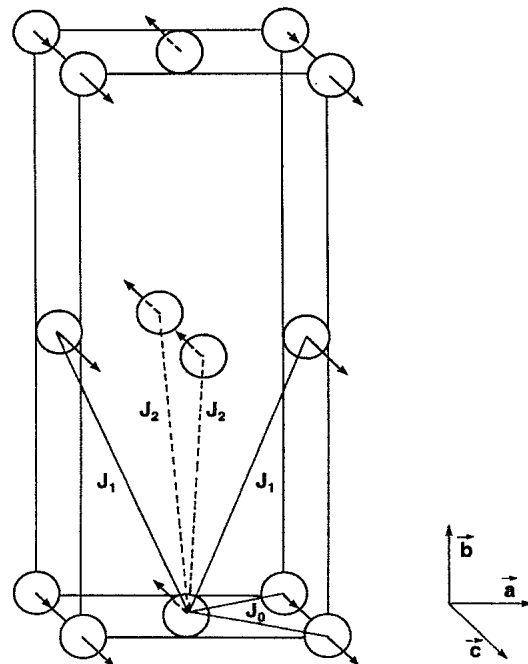


FIG. 1. Illustration of the spin structure of antiferromagnetic La_2CuO_4 . Only copper sites in the orthorhombic cell are shown. All three interactions are antiferromagnetic and $|J_0| \gg |J_1|, |J_2|$.

In this paper we have applied mean-field theory, the spin-wave theory, and Monte Carlo (MC) simulations to study the magnetic ordering in orthorhombic quasi-two-dimensional antiferromagnets such as K_2NiF_4 ,⁶ La_2CuO_4 , and La_2NiO_4 .⁷ Because the coupling in the CuO planes is so large, we have used a renormalized mean-field theory, in which the properties of the spins in the two-dimensional planes are treated exactly but are coupled only by a mean field to spins in neighboring planes. That produces a value for T_N which depends only on the net coupling ΔJ and not on the individual values J_1 and J_2 as long as $|J_1| \leq 0.8|J_0|$. To check this simple theory, we have carried out extensive Monte Carlo simulations on systems of size up to 18 000 spins. We find that while T_N depends only on ΔJ , the renormalized mean-field theory overestimates T_N by a factor of 2–3 depending on ΔJ . Since the exact 2D χ entering this mean-field theory is close to the in-plane χ of the 3D simulations, this error can arise only from the omission of interplane correlations and the attendant fluctuations.

We also carried out a low-temperature spin-wave calculation for T_N . Because only the net coupling between planes is important, we simplified the calculation by studying the anisotropic Heisenberg model on a simple cubic lattice. We generalized the analysis of Takahashi,⁸ who studied the isotropic case, to include anisotropic interactions. In this approach, T_N is like a Bose-Einstein condensation temperature below which long-range order results. We find this theory agrees fairly well with our simulations over a wide range of coupling ΔJ .

In Sec. II we describe the model and our simulation procedure. In Sec. III, we present results for both the renormalized mean-field theory and for our simulations. The results from the spin-wave calculation for anisotropic systems is presented in Sec. IV. A summary of our results as well as a comparison with experimental results is presented in Sec. V. Finally, we present details of the spin-wave theory in the Appendix.

II. MODEL AND METHODS

We have studied the classical antiferromagnetic Heisenberg model on a face-centered orthorhombic lattice, Fig. 1. This model represents the Cu spins in the undoped La_2CuO_4 compounds. The nearest-neighbor coupling J_0 in the a - c plane is antiferromagnetic and quite strong, $J_0 \approx 1300$ K. The two couplings between the planes, J_1 and J_2 , are also antiferromagnetic, but much weaker than J_0 . The Hamiltonian of this model is

$$H = - \sum_{a-c} J_0 \mathbf{s}_i \cdot \mathbf{s}_j - \sum_{a-b} J_1 \mathbf{s}_i \cdot \mathbf{s}_j - \sum_{b-c} J_2 \mathbf{s}_i \cdot \mathbf{s}_j, \quad (1)$$

where \mathbf{s}_i can point in any direction but has magnitude 1. Here the summations are over the nearest-neighbor spin pairs in the a - c , a - b , and b - c planes, respectively, and negative coupling J_{ij} represents an antiferromagnetic interaction. In the orthorhombic state, J_1 and J_2 are not equal, and we can define $\Delta J = |J_1| - |J_2|$ and define temperature in units of $|J_0|$.

We used the Monte Carlo method to study this model.⁹

For simulations on our IBM 3090/180 computer, a spin was chosen at random and rotated by a small random amount subject to a heat-bath algorithm which we used to determine whether to accept the change. The new spin direction was determined as the following, $\mathbf{s}_i \rightarrow (\mathbf{s}_i + \mathbf{R}) / |\mathbf{s}_i + \mathbf{R}|$, where \mathbf{R} is a random vector with a fixed length $|\mathbf{R}|$. The energy change ΔE was then calculated and the spin flipped with probability $e^{-\Delta E/kT} / (1 + e^{-\Delta E/kT})$. The $|\mathbf{R}|$ was chosen so that the acceptance ratio of change was between 0.4 and 0.6. One Monte Carlo step (MCS) was defined as N attempted spin moves where N is the number of spins in the system. We also carried out simulations on a Cray-XMP supercomputer for our largest samples. To utilize the vector nature of the Cray, we divided the total spins into four groups with $N/4$ spins each (in each group, there are no nearest-neighbor spins). We then attempted to flip each group at one step, using the same heat-bath algorithm to determine whether the move would be accepted or not. In this modified parallel process, we gained a factor of 10 on the speed. In all of our simulations, we used periodic boundary conditions in all three spatial directions. We studied samples with sizes $N=600$ ($10 \times 10 \times 6$), 4000 ($20 \times 20 \times 10$) and 18 000 ($30 \times 30 \times 20$), with the larger dimensions in the a - c plane, though most simulation runs were on $N=18 000$.

When $\Delta J=0$ the system is highly degenerate because one can reverse all the spins in one layer without changing the energy. When $\Delta J \neq 0$, the model is nondegenerate (aside from the global rotational symmetry), and at $T=0$ has long-range ferromagnetic order in the b - c plane and antiferromagnetic (AF) ordering along a (since $|J_1| > |J_2|$, AF ordering is more favorable along a). With this convention, we can define the staggered magnetization \mathbf{M}_s ,

$$\mathbf{M}_s = \frac{1}{N} \sum_i \mathbf{s}_i e^{iq \cdot \mathbf{r}_i}, \quad (2)$$

where $\mathbf{q} = (2\pi/a)(1,0,0)$ and ordinary magnetization $\mathbf{M} = (1/N) \sum_i \mathbf{s}_i$. In the ground state $\mathbf{M}_s = 1$ and $\mathbf{M} = 0$. M_s is the order parameter which can be used to describe the order-disorder transition. Along this line we can define the staggered susceptibility χ_s as

$$\chi_s = (\langle M_s^2 \rangle - \langle M_s \rangle^2) / T, \quad (3)$$

where $M_s^2 = \mathbf{M}_s \cdot \mathbf{M}_s$ and $\langle M_s \rangle \equiv \langle |\mathbf{M}_s| \rangle$. Because of the global rotational symmetry of the spins and the finite sample size, it is more appropriate to average over amplitudes than over the vector itself. The ground-state energy per spin is $E_g = 2J_0 - 2\Delta J$.

We used $|\mathbf{M}_s|$ to determine the AF to paramagnetic transition or Néel temperature T_N . In most of the runs, we started from the ground state and increase the temperature slowly. For temperatures far from the transition, we have averaged 2000 MCS per temperature after allowing 500 MCS to equilibrium. Near the critical region, we have typically run 10 000 MCS per temperature. To be sure the system was in equilibrium near the transition, we made runs in which we have increased the temperature slowly to $T \approx 2T_N$ and then decreased the temperature to

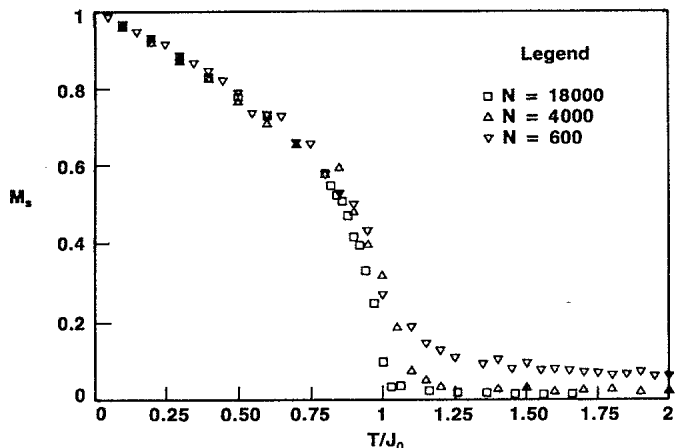


FIG. 2. Staggered magnetization $|M_s|$ vs temperatures T/J_0 for three sample sizes. For $N=4000$ and $N=18000$, the results are almost identical.

below T_N . Both paths gave the same transition temperature within a few percent.

To test the finite-size effect, we ran several samples with the same J 's but different sizes, as shown in Fig. 2. We see that there is little difference between runs for 4000 and 18000 spins. Thus the results of our runs, most of which have been on $N=18000$ systems, should give a reasonable estimate for T_N , accurate to within a few percent.

III. RESULTS

The first interesting result we have is that the transition temperature T_N depends only on the difference of the two interplane couplings, when both J_1 and J_2 are much smaller than J_0 , as shown in Fig. 3. For different pairs of J_1 and J_2 , and fixed ΔJ , the curves for M_s are nearly identical for $|J_1| < 0.8|J_0|$. Thus we can see that the transition temperature depends only on ΔJ . This result is in agreement with the mean-field calculation, where the 3D Néel temperature only depends on the 2D

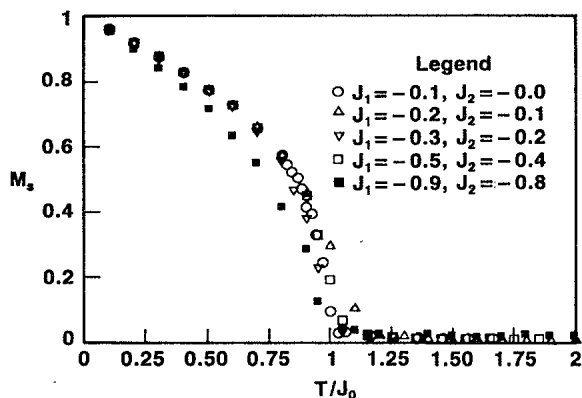


FIG. 3. Staggered magnetization $|M_s|$ as a function of temperature T/J_0 for different pairs of interactions J_1 and J_2 , but with same $\Delta J=0.1$. Note that T_N depends only on the ΔJ , except for $J_1=0.9, J_2=0.8$, where T_N is slightly suppressed.

susceptibility and the net coupling between the planes, provided the interplane coupling is small. We have also calculated the energy per spin, specific heat, M_s , and staggered susceptibility as functions of temperature. These are shown in Fig. 4 for $\Delta J=0.1$. The peaks in the specific heat and the staggered susceptibility curves give a clear indication of the phase transition at the Néel temperature T_N .

For different values of ΔJ , we show a sequence of M_s 's in Fig. 5. As ΔJ increases, T_N increases since the net interplane interaction each spin feels favors the antiferromagnetic state. As ΔJ decreases, the spin-correlation length increases in the a - c plane and become very much larger than our sample size before T_N is reached. Thus the smallest ΔJ we can study is limited by the finite size of our sample when the correlation length in the a - c plane is the same order as the sample size. Obviously, when $\Delta J=0$, there is no net interaction between planes. The system should behave as a set of uncoupled 2D antiferromagnetic Heisenberg models, which are known to have a zero transition temperature. To test this idea, we simulated a model with $\Delta J=0$ ($J_2=J_1=0.1J_0$). After starting the system in its ground state ($M_s=1$), we heated the system up slowly to $T=1.0J$, where $M_s=0$, and then cooled the system back down to low temperatures. The

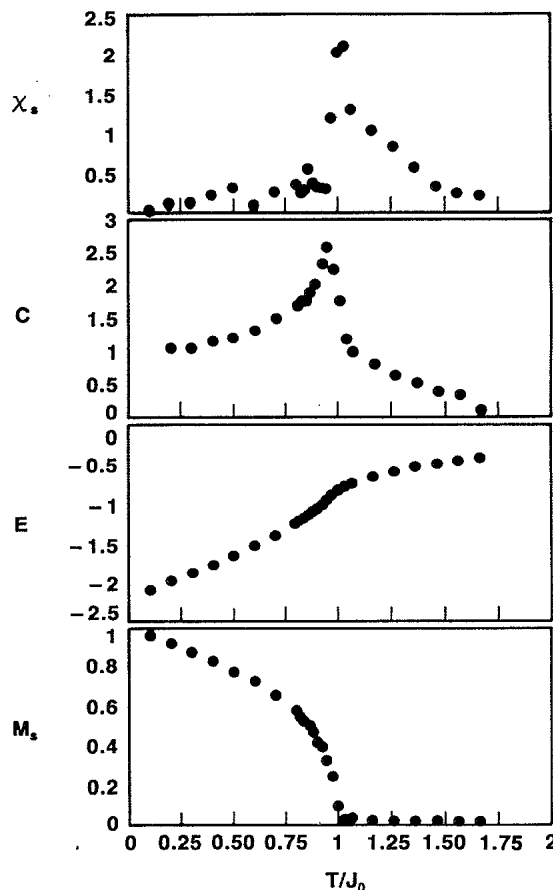


FIG. 4. Temperature dependence of the staggered magnetization M_s , the staggered susceptibility χ_s , energy per spin E , and the specific heat $C=dE/dT$ for $\Delta J=0.1$ and $N=18000$.

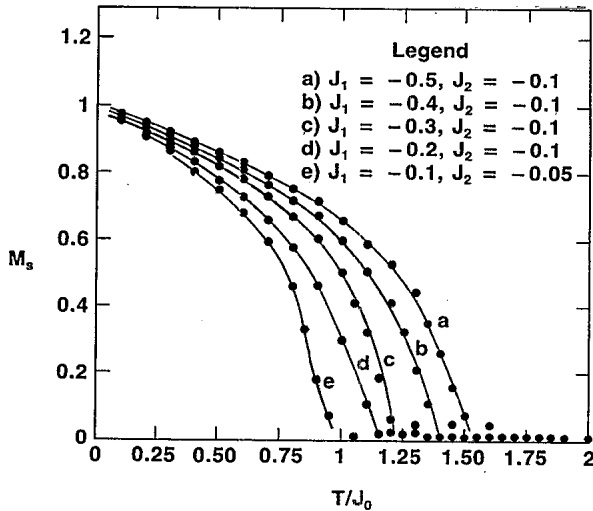


FIG. 5. Staggered magnetization vs temperature T/J_0 for different values of ΔJ . Note that as ΔJ increases, T_N also increases since the net antiferromagnetic interaction between spins is increased.

staggered magnetization M_s remains close to zero (not as in the case with a finite transition temperature in which M_s increases as the temperature is lowered below T_N).

The relation between the T_N and the ΔJ is very important, and results from our simulation are shown in Fig. 6. T_N increases rapidly as ΔJ increases for small ΔJ , but for $\Delta J > 0.1$, T_N is nearly linear with ΔJ .

To understand this behavior of T_N , one can carry out a simple mean-field calculation in which the field that each spin feels is just determined from the sum of its interactions with its neighbors. For a Heisenberg model, this gives $T_N = \frac{2}{3} (-\sum_i J_i)$, and thus we have for our model, $T_N = (-4J_0 + 4\Delta J)/3$. For the case $\Delta J = 0.1$, this result gives $T_N = 1.47 |J_0|$, which is much higher than from our simulation. Obviously for ΔJ small, this simple mean-field approach is not good since it does not correctly take into account the strong fluctuations which destroy long-range order in the limit $\Delta J \rightarrow 0$.

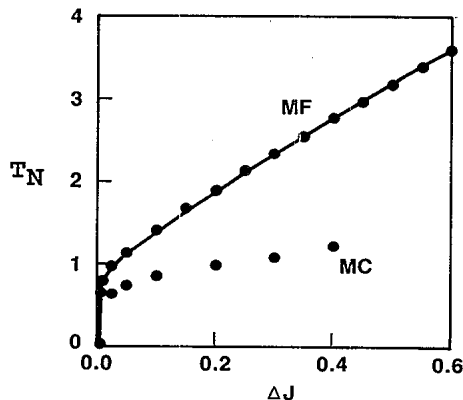


FIG. 6. Néel temperature T_N as a function of the interplane coupling ΔJ . The lower curve is the Monte Carlo result while the upper curve is determined from the renormalized mean-field theory Eq. (6).

We notice that if we put $J_1 = J_2 = 0$, then this model becomes a 2D antiferromagnetic Heisenberg model, and the susceptibility χ_s becomes χ_s^{2D} . When ΔJ is small and since only ΔJ is important in determining T_N , one might try a renormalized mean-field theory¹⁰ taking into account the fact that χ_s^{2D} is known. Each plane has a 2D susceptibility χ_s^{2D} , the coupling between the planes is just the net interaction each spin feels, which is $4\Delta J$. (Since we have eight neighbors, there are four pairs ΔJ .) Thus we have for all orders of interactions

$$\chi_s = \chi_s^{2D} + \chi_s^{2D} 4\Delta J \chi_s^{2D} + \dots \quad (4)$$

After the geometric summation, we find

$$\chi_s = \chi_s^{2D} / (1 - 4\chi_s^{2D} \Delta J), \quad (5)$$

where χ_s^{2D} is the susceptibility for the 2D AF Heisenberg model. At the Néel temperature, the susceptibility diverges, and the expected transition temperature can be obtained from

$$4\chi_s^{2D}(T_N)\Delta J = 1. \quad (6)$$

This result can also be obtained straightforwardly simply by factorizing the interaction between spins in different planes but treating interactions within planes exactly.

From earlier studies on the 2D Heisenberg model, we know how χ_s^{2D} behaves as a function of temperature. By using the high-temperature expansion result for χ_s^{2D} for ($T > 0.8$) and spin-wave theory for lower temperature, we can obtain results for T_N for different ΔJ 's. The upper curve in Fig. 6 is the renormalized mean-field result, while the lower curve corresponds to our Monte Carlo result. For $T > 0.8$, the correlation length for the 2D Heisenberg model is smaller than our sample size, and finite-size effects are not important. We can see that the mean-field curve is higher than the Monte Carlo simulation, and, at $\Delta J = 0.1$, the difference is about a factor of 3.

While it is easy to understand why this renormalized mean-field theory breaks down for large ΔJ , it is somewhat surprising that it does not work well in the range of ΔJ of interest. One reason for the discrepancy could be the suppression of the 2D fluctuations by the interplane interaction. Since it is the 2D fluctuations which lead to large χ_{2D} , the susceptibility is thereby reduced and thence T_N . To investigate this point, we calculated the in-plane susceptibility $\bar{\chi}_s^{2D}$ in our model for $T > T_N$,

$$T\bar{\chi}_s^{2D} = \frac{1}{N_{2D}} \left\langle \sum_i \langle \mathbf{M}_{s,i}^{2D} \cdot \mathbf{M}_{s,i}^{2D} \rangle \right\rangle_{\text{layer}}, \quad (7)$$

where $\langle \rangle_{\text{layer}}$ represents an average over the layers, and \mathbf{M}_s^{2D} is the staggered magnetization in one layer. In Fig. 7, for $\Delta J = 0.1$, we can see that there is a slight suppression of the χ_s^{2D} at high temperature. At low temperature due to the ordered phase in the 3D model, $\bar{\chi}_s^{2D}$ diverges below T_N . But the amount of suppression is small and not enough to make a factor of 3 difference in the estimated T_N . Indeed, χ_s^{2D} and $\bar{\chi}_s^{2D}$ are essentially equal at the mean-field result for T_N . The simple renormalized mean-field result, Eq. (5), is thus not valid for the range of

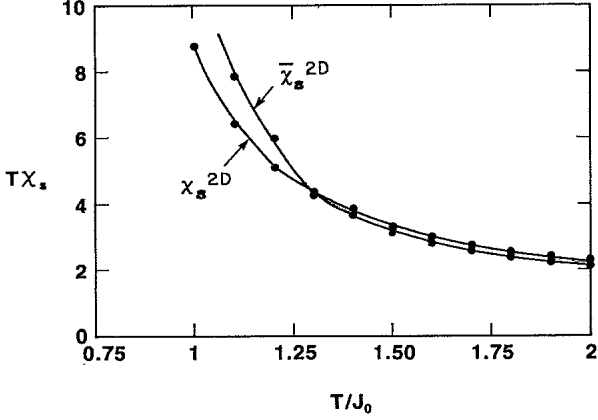


FIG. 7. The 2D susceptibility $T\chi$, Eq. (7) in the 3D model, compared with true 2D χ_{2D} determined from high-temperature series expansion for the 2D Heisenberg model. At low temperature, due to the ordering $\bar{\chi}_{2D}$ as well as χ_{3D} , diverges, while at high temperature, the $\bar{\chi}_{2D}$ get suppressed slightly from χ_{2D} .

ΔJ studied here, most probably because of the neglect of short-range interplane correlations caused by the relatively large values of ΔJ explored here. At lower temperatures, the exponential dependence of $\chi_s^{2D} \approx \exp(4\pi/T)$ in the classical Heisenberg model continues to lead to overestimation of T_N for small ΔJ . For example, to obtain $T_N \approx 0.1$ (as found in the experiments), requires ΔJ to have the unrealistically small value of 10^{-45} for χ_s^{2D} from spin-wave theory or 10^{-43} for χ_s^{2D} from the more accurate Shenker and Tobochnik¹¹ formula. Of course, it is the spin- $\frac{1}{2}$ quantum Heisenberg model which applies to the real materials. A simple quantum spin-wave calculation for χ yields the result $\chi \propto \exp[4\pi s(s+1)/T]$. Since $s(s+1)$ is $\frac{3}{4}$ instead of unity as in the classical case, the value of ΔJ increases somewhat to 10^{-31} for $T=0.1$. A recent quantum Monte Carlo simulation¹² suggests, on the other hand, that χ diverges even more strongly than the classical result, a result which we reject as incorrect. An interesting possible explanation is that proposed by Chakravarty *et al.*¹³ that zero-point fluctuations reduce the factor multiplying $4\pi/T$ in the exponential below $s(s+1)$, a point we shall return to in the conclusions, Sec. V.

From our results above, we can see that the Néel temperature depends only on the $\Delta J = J_1 - J_2$, so it is not necessary for J_1 and J_2 to be antiferromagnetic. Both J_1 and J_2 could in fact be ferromagnetic, as long as ΔJ is kept fixed. To see how this would affect experimentally measurable quantities, we carried out additional simulations for two situations: (i) J_1, J_2 ferromagnetic and (ii) J_1, J_2 antiferromagnetic, with $\Delta J = 0.1$. We found that both the staggered magnetization and the specific heat are unchanged, and the only quantity which shows any difference is the regular susceptibility defined as

$$T\chi = \frac{1}{N} \sum_i \langle M_i^2 \rangle \quad (8)$$

as shown in Fig. 8. Clearly the ferromagnetic model has

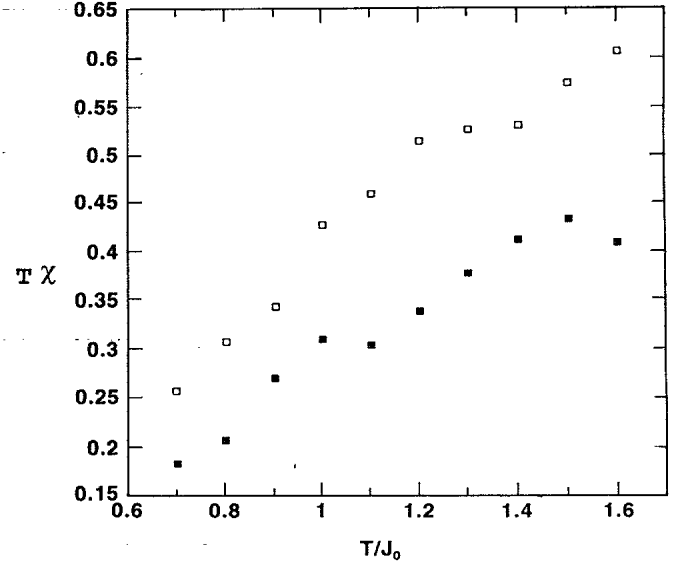


FIG. 8. $T\chi$ as a function of T for both cases; (i) both J_1, J_2 are antiferromagnetic and (ii) both J_1, J_2 are ferromagnetic with the same value of $\Delta J = 0.1$. The susceptibility is slightly larger when both interactions are ferromagnetic.

a χ larger than the antiferromagnetic case. However, neither $T\chi$ shows the anomalous behavior near T_N as exhibited by the experimental data.¹⁴

IV. LOW-TEMPERATURE SPIN-WAVE CALCULATION

When the interplane coupling ΔJ is small, this model can be approximated by a Heisenberg model on a simple cubic lattice, with in-plane interaction J and interplane interaction J' , since T_N depends only on ΔJ . The Hamiltonian for this simple cubic model is

$$H = -J \sum_{i,j} \mathbf{s}_i \cdot \mathbf{s}_j - J' \sum_{i,j} \mathbf{s}_i \cdot \mathbf{s}_j, \quad (9)$$

where the first sum is over four nearest neighbors in the plane and the second sum is over the nearest-neighbor interplane interactions. On the simple cubic lattice, we can carry out a simple gauge transformation and treat the spin interactions as ferromagnetic, in which case $J = |J_0|$ and $J' = 2\Delta J$. This makes the spin-wave analysis easier. The ratio of the two interactions $J'/J = \gamma$ should determine the transition temperature of the model. When $\gamma = 0$, we have a two-dimensional model with no interplane interactions, and the transition temperature is zero. When $\gamma = 1$, we recover a simple cubic Heisenberg model with equal interactions,¹⁵ for which the transition temperature is known to be $T_c = 1.35$. We also did some MC simulations on the anisotropic simple cubic model, and found that the transition temperatures almost identical to that on the orthorhombic lattice with $J' = 2\Delta J$.

Following Takahashi,⁸ we can treat our classical spin system, with in-plane ferromagnetic interaction J and interplane interaction $J' < J$, by using modified spin-wave theory. The details of the derivation are given in the Appendix. The result is shown in Fig. 9. In the temperature range of our Monte Carlo simulation, the spin-wave

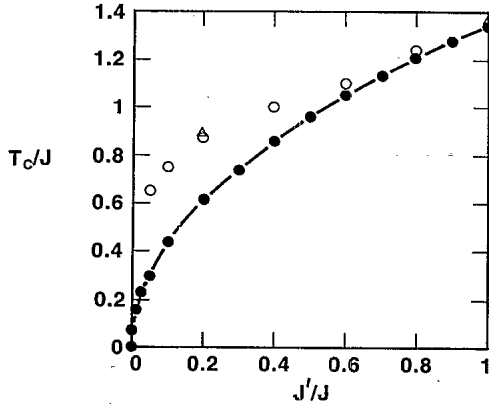


FIG. 9. Results for the transition temperature T_c/J from the low-temperature spin-wave theory (solid circles) vs $\gamma = J'/J$ and results from the simulations on the simple cubic lattice (triangles) and on the orthorhombic lattice (open circles) with $J' = 2\Delta J$.

theory on the simple cubic lattice can produce a much better solution than the mean-field theory, although the spin-wave Néel transition temperatures are not quite the same as in our Monte Carlo simulations. For $T_c \approx 0.1$ we found a value of $\Delta J = 10^{-3}$ for $T_c = 0.1$. Note that a similar calculation is possible for the LaCuO_2 orthorhombic lattice, but it requires solving three simultaneous integral equations. Here we ignored the small orthorhombic distortions and only considered the simpler case.

V. CONCLUSIONS AND DISCUSSION

Through our Monte Carlo simulations on the classical Heisenberg spin system on the orthorhombic lattice, we have found that the Néel temperature for the antiferromagnetic-to-paramagnetic transition depends only on the difference of the two interplane interactions, ΔJ . In the temperature range $T > 0.5$, the mean-field theory result is a factor of 3 higher in estimating T_N . The error occurs in part because the 2D fluctuations increasing the 2D staggered susceptibility are suppressed by the interplane interactions even for small interactions. In this temperature range, a Heisenberg model on the simple cubic lattice with interplane interaction $J' = 2\Delta J < J$ gives a reasonable approximation. The improvement results from taking into account the increasingly 3D character of the fluctuations. At the lower temperatures of interest for smaller interplane interactions, the correlation length is much larger than the sample size we can handle using Monte Carlo techniques. In this temperature range, we are forced to rely on the anisotropic simple cubic spin-wave theory.

While the calculations above are applicable to any system of spins strongly coupled in two dimensions but weakly coupled in the third dimension, the application to La_2CuO_4 is complicated by the fact that this system has recently been found¹⁶ to have a weak antisymmetric in-plane exchange of the Dzyaloshinsky-Moriya form.¹⁷ This gives us to a very small ferromagnetic in-plane coupling and is necessary to explain the "peak" seen in the temperature dependence of χ below T_N .³ The results

presented here may be more applicable to the $\text{YBr}_2\text{Cu}_3\text{O}_{6+x}$ antiferromagnets.

It is interesting that the renormalized mean-field theory gives values of T_N which are too high for $T_N > 0.5$ by a factor of 3, whereas Chakravarty *et al.*¹³ and Thio *et al.*¹⁶ have found that a renormalized mean-field theory using an accurate treatment of χ_{2D} for the spin- $\frac{1}{2}$ Heisenberg model gives a quantitative, internally-consistent picture of the observed in-plane coherence length, spin-wave speed, T_N , and uniform-field susceptibility in La_2CuO_4 . Why does mean-field theory work for the spin- $\frac{1}{2}$ case and fail for the classical case? One can argue that the consistent picture developed by these authors is insensitive to variations of a factor of 3 in T_N . Effective decoupling of adjacent 2D planes by the quantum zero-point spin fluctuations is a more plausible explanation.

Chakravarty *et al.*¹³ find a value of ΔJ of $\sim 10^{-5} |J_0|$. Assuming that J_1 and J_2 have an exponential dependence on atomic position, with a decay distance of order a typical ionic radius for the species involved in the superexchange, we can estimate ΔJ as $|J_1| (\Delta u/a)$, where Δu is the difference in Cu-Cu separation between interaction 2 and interaction 1. The observed value of $\Delta u/a$ of $\sim 10^{-2}$ implies that $|J_1| \sim 10^{-3} |J_0|$ or of that order. Is this small value of $|J_1|$ reasonable when $|J_0|$ is as large as 1300 K in the light of conventional superexchange theory. Considering that J_1 arises from a sixth-order process and that many comparable values of superexchange are known, we conclude that such a value is reasonable. On the other hand, J_0 arises from a fourth-order process in the Mott-Hubbard insulating limit. Using values of the transfer integral taken from the band calculations¹⁸ and standard fourth-order theory, one is forced to conclude that the effective U for the Cu $d_{x^2-y^2}$ orbital is about an order of magnitude smaller than the bare Cu U and that one is quite close to the Mott-Hubbard transition. For $\text{La}_2\text{BaCuO}_4$, however, it would be more accurate to think of the transition as a hybridization-dehybridization transition.

A value of $\Delta u/a$ of $\sim 10^{-2}$ is of order of or smaller than amplitudes of atomic vibration at T_N , and the variation of ΔJ caused by the vibrations of the atoms involved in the superexchange can be significantly larger than the mean value $\Delta J = |J_1| (\Delta u/a)$ irrespective of the value one assigns to $|J_1|$. This concern, which could in principle invalidate the approaches of Chakravarty *et al.*,¹³ and of the present paper, can be put aside after one realizes that all of the modes affecting the relative displacement of the atoms involved in J_1 and J_2 are optical modes involving oxygen and therefore of relatively high frequency. Motional narrowing thus eliminates any significant effect of the thermal or dynamical disorder in J_1 and J_2 , leaving only the mean value of ΔJ , $|J_1| \Delta u/a$, of importance.

APPENDIX

We used a modified spin-wave theory to calculate the order-disorder transition temperature of a classical spin system on a simple cubic lattice with $J'/J = \gamma < 1$. We

begin with the quantum version of Eq. (9), replacing s_i by S_i to denote quantum spins. We follow the derivation by Takahashi who studied the case $\gamma=1$ and apply the Holstein-Primakoff transformation to order S^{-1} , where S is the magnitude of spin S_i . The product operator $S_i \cdot S_j$ is then expressed as follows:

$$S_i \cdot S_j = S^2 - S(a_i^* - a_j^*)(a_i - a_j) - \frac{1}{4}[a_i^* a_j^* (a_i - a_j)^2 + (a_i^* - a_j^*) a_i a_j] + O(S^{-1}), \quad (A1)$$

where a_j^* and a_j are the creation and annihilation operators of bosons at the j th site. Following Takahashi, we can define the ideal spin-wave density matrix:

$$\rho = C \exp \left[- \sum_k g(k) a_k^* a_k \right]. \quad (A2)$$

$$0 = \frac{\partial W}{\partial g(k)} = \frac{\exp[g(k)]}{\{\exp[g(k)] - 1\}^2} \left[-JS'_1 \sum_i [1 - \cos(\mathbf{k} \cdot \delta_1)] - J'S'_2 \sum_i [1 - \cos(\mathbf{k} \cdot \delta_2)] + Tg(k) - \mu \right], \quad (A6)$$

$$S'_i = S - \frac{1}{N} \sum_k [1 - \exp(i\mathbf{k} \cdot \delta_i)] \bar{n}_k,$$

where $i=1,2$ and $\varepsilon_i(k) = \sum_i [1 - \cos(\mathbf{k} \cdot \delta_i)]$, μ is the Lagrange multiplier, δ_1 is the lattice vectors to nearest neighbors in the plane, and δ_2 is the lattice vector to the nearest interplane neighbors. Now we have three coupled equations for three unknowns, S'_1, S'_2 , and μ ,

$$S = \frac{1}{N} \sum_k \left[\exp \left[\frac{JS'_1 \varepsilon_1 + J'S'_2 \varepsilon_2 - \mu}{T} \right] - 1 \right]^{-1}, \quad (A7)$$

$$S'_1 = \frac{1}{N} \sum_k \frac{\cos(\mathbf{k} \cdot \delta_1)}{\exp[(JS'_1 \varepsilon_1 + J'S'_2 \varepsilon_2 - \mu)/T] - 1}, \quad (A8)$$

$$S'_2 = \frac{1}{N} \sum_k \frac{\cos(\mathbf{k} \cdot \delta_2)}{\exp[(JS'_1 \varepsilon_1 + J'S'_2 \varepsilon_2 - \mu)/T] - 1}. \quad (A9)$$

By taking the limit of infinite S , we can treat the classical case. Replacing J and J' by J/S^2 and J'/S^2 , setting $S_i/S = S_i$, and expanding the exponentials in (A7)–(A9) we can rewrite Eqs. (A7)–(A9) in the form

$$\frac{x_1}{t} = \frac{1}{N} \sum_k [\varepsilon_1(k) + \gamma r \varepsilon_2(k) - \mu S / Jx_1]^{-1}, \quad (A10)$$

$$\frac{x_1^2}{t} = \frac{1}{N} \sum_k \frac{\cos(\mathbf{k} \cdot \delta_1)}{\varepsilon_1(k) + \gamma r \varepsilon_2(k) - \mu S / Jx_1}, \quad (A11)$$

$$\frac{x_1 x_2}{t} = \frac{1}{N} \sum_k \frac{\cos(\mathbf{k} \cdot \delta_2)}{\varepsilon_1(k) + \gamma r \varepsilon_2(k) - \mu S / Jx_1}, \quad (A12)$$

where $x_1 = S'_1/S$, $x_2 = S'_2/S$, $\gamma = J'/J$, $t = T/J$, and $r = x_2/x_1 = S_2/S_1$. Since $\mu < 0$, the condition $S_z = 0$ cannot always be satisfied at low temperatures. At critical temperature T_c , we obtain a phase transition to states with $S_z \neq 0$. As in Bose-Einstein condensation, T_c is

The expectation value of $S_i \cdot S_j$ then becomes

$$\text{Tr} \rho S_i \cdot S_j / \text{Tr} \rho = \left| S - \frac{1}{N} \sum_k (1 - e^{i\mathbf{k} \cdot \mathbf{r}_{ij}}) \bar{n}_k \right|^2, \quad (A3a)$$

$$\bar{n}_k = \{\exp[g(k)] - 1\}^{-1}. \quad (A3b)$$

The entropy \mathcal{S} and magnetization S_z are then given by

$$\mathcal{S} = \sum_k \frac{g(k)}{\exp[g(k)] - 1} - \ln\{1 - \exp[-g(k)]\}, \quad (A4)$$

$$S_z = SN - \sum_k n_k = 0. \quad (A5)$$

Minimizing the free energy $W = E - \mathcal{S}T$ with respect to $g(k)$ under the condition $S_z = 0$ gives

defined by the condition $\mu = 0$. Therefore, at T_c , we have

$$x_1/t = N^{-1} \sum_k [\varepsilon_1(k) + \gamma r \varepsilon_2(k)]^{-1}, \quad (A13)$$

$$x_1^2/t = N^{-1} \sum_k [1 - \varepsilon_1(k)/4][\varepsilon_1(k) + \gamma r \varepsilon_2(k)]^{-1}, \quad (A14)$$

$$x_1 x_2/t = N^{-1} \sum_k [1 - \varepsilon_2(k)/2][\varepsilon_1(k) + \gamma r \varepsilon_2(k)]^{-1}. \quad (A15)$$

In the limit of large systems, the sum in Eqs. (A14)–(A16) can be replaced by integrals. For the simple cubic lattice it is straightforward to carry out the integrals over k_x and k_y , and Eqs. (A13)–(A15) can then be written as

$$x_1/t_c = I_1(\gamma, r), \quad (A16)$$

$$x_1^2/t_c = \frac{1}{2}(2 + \gamma r)I_1(\gamma, r) - (\gamma r/2)I_2(\gamma, r) - \frac{1}{4}, \quad (A17)$$

$$x_1 x_2/t_c = I_2(\gamma, r), \quad (A18)$$

where

$$I_1(\gamma, r) = \frac{1}{(2\pi)^2} \int_0^{2\pi} dz k K(k),$$

$$I_2(\gamma, r) = \frac{1}{(2\pi)^2} \int_0^{2\pi} dz \cos(z) k K(k), \quad (A19)$$

$$k = \{1 + (\gamma r/4)[2 - 2\cos(z)]\}^{-1},$$

and $K(k)$ is the complete elliptic integral of the first kind. These expressions can be combined to eliminate r , and then solved numerically to give T_c as a function of γ as shown in Fig. 9.

- ¹D. Vaknin, S. K. Sinha, D. E. Moncton, D. C. Johnston, J. M. Newsam, C. R. Safinya, and H. E. King, Jr., *Phys. Rev. Lett.* **58**, 2802 (1987).
- ²T. Freltoft *et al.*, *Phys. Rev. B* **36**, 826 (1987).
- ³D. C. Johnston, J. P. Stokes, D. P. Goshorn, and J. T. Lewandowski, *Phys. Rev. B* **36**, 4007 (1987).
- ⁴S. K. Sinha, D. E. Moncton, D. C. Johnston, D. Vaknin, G. Shirane, and C. Stassis, *Phys. Rev. Lett.* (to be published).
- ⁵G. Shirane *et al.*, *Phys. Rev. Lett.* **59**, 1613 (1987); Y. Endoh *et al.*, *Phys. Rev. B* (to be published).
- ⁶R. J. Birgeneau, J. Als-Nielsen, and G. Shirane, *Phys. Rev. B* **16**, 280 (1977).
- ⁷G. Aeppli and D. J. Bultrey (unpublished).
- ⁸M. Takahashi, *Phys. Rev. B* **36**, 3791 (1987).
- ⁹R. E. Watson, M. Blume, and G. H. Vineyard, *Phys. Rev. B* **2**, 684 (1970).
- ¹⁰A. Aharony, R. J. Birgeneau, A. Coniglio, M. A. Kastner, and H. E. Stanley, *Phys. Rev. Lett.* **60**, 1330 (1988).
- ¹¹S. Shenker and J. Tobochnik, *Phys. Rev. B* **22**, 4462 (1980).
- ¹²E. Manousakis and R. Salvador, *Phys. Rev. Lett.* **60**, 840 (1988); J. D. Reger and A. P. Young, *Phys. Rev. B* (to be published).
- ¹³S. Chakravarty, B. I. Halperin, and D. R. Nelson, *Phys. Rev. Lett.* **60**, 1057 (1988).
- ¹⁴M. A. Kastner *et al.*, *Phys. Rev. B* **37**, 111 (1988).
- ¹⁵T. Thio *et al.* (unpublished).
- ¹⁶H. Bastuyaku, *Phys. Lett.* **65A**, 98 (1977); M. A. Klenin, *Phys. Rev. B* **19**, 3586 (1979).
- ¹⁷Band-structure calculation, e.g., J. Yu, A. J. Freeman, and J. H. Xu, *Phys. Rev. Lett.* **58**, 1035 (1987).
- ¹⁸I. E. Dzyaloshinsky, *J. Phys. Chem. Solids* **4**, 241 (1958); T. Moriya, *Phys. Rev. Lett.* **4**, 5 (1960).